PLASMA FOCUSING OF HIGH ENERGY DENSITY ELECTRON AND POSITRON BEAMS *

J.S.T. Ng, P. Chen, W. Craddock, F.J. Decker, R.C. Field, R. Iverson, F. King,
R.E. Kirby, P. Raimondi, D. Walz, SLAC, Stanford, CA. 94309, USA
H.A. Baldis†, P. Bolton, LLNL, Livermore, CA. 94551, USA
D. Cline, Y. Fukui, V. Kumar, UCLA, Los Angeles, CA. 90024, USA
C. Crawford, R. Noble, FNAL, Batavia, IL. 60510, USA
K. Nakajima, KEK, Tsukuba, Ibaraki 305-0801, Japan
A. Ogata, Hiroshima University, Kagamiyama, Higashi-Hiroshima, 739-8526 Japan
A.W. Weidemann, University of Tennessee, Knoxville, Tennessee 37996, USA

Abstract

We present results from the SLAC E-150 experiment on plasma focusing of high energy density electron and, for the first time, positron beams. We also discuss measurements on plasma lens-induced synchrotron radiation and laser- and beam-plasma interactions.

1 INTRODUCTION

The plasma lens was proposed as a final focusing mechanism to achieve high luminosity for future high energy linear colliders [1]. Previous experiments to test this concept were carried out with low energy density electron beams [2]. The goals of the SLAC E-150 experiment are to study plasma focusing for high energy, high density particle beams in the regime relevant to linear colliders, to obtain better understanding of beam-plasma interactions, and to bench-mark computer codes for plasma lens designs. Such studies will help to develop compact and economical plasma lens designs suitable for collider experiments. In this paper, we present results obtained by the E-150 collaboration on plasma focusing of high energy density electron and positron beams.

2 EXPERIMENTAL SETUP

The experiment was carried out at the SLAC Final Focus Test Beam facility (FFTB)[3]. The experiment operated parasitically with the PEP-II B-factory; the high energy electron and positron beams were delivered to the FFTB at 1 - 10 Hz from the SLAC linac. The beam parameters are summarized in Table 1.

A layout of the beam line is shown in Figure 1. The beam size was measured using a wire scanner system. A carbon fiber 7 μm in diameter was placed downstream of the plasma lens, adjustable along the beam axis in a range of 8 to 30 mm from the center of the lens. The Bremsstrahlung photons were detected 35 m downstream by an air-Cherenkov detector. The synchrotron radiation monitor, consisting of a stack of ionization chambers interleaved with polyethylene blocks, was installed 33 m downstream, in front of the Cherenkov detector. This detector was used to monitor the synchrotron radiation emitted as a result of the strong bending of the beam particles by the plasma lens. It provided an independent measure of the focusing strength. A toroid located just in front of the electron/positron beam dump was used to monitor the bunch charge.

To create the plasma lens, a short burst (800 μs duration) of neutral nitrogen or hydrogen gas, injected into the plasma chamber by a fast-pulsing nozzle, was ionized by an infrared laser and/or the high energy beam. The neutral density was determined by interferometry to be 4×10^{18} cm^{-3} for N_2 at a plenum pressure of 1000 psi. The injected gas was evacuated by a differential pumping system which made operation of the gas jet possible while maintaining ultra-high vacuum in the beam lines on either side of the chamber.

Table 1: FFTB electron and positron beam parameters for this experiment.

Parameter	Value
Bunch intensity	1.5×10^{10} particles per pulse
Beam size	5 to 8 μm (X),
	3 to 5 μm (Y)
Bunch length	0.7 mm
Beam energy	29 GeV
Normalized emittance	3 to 5 $\times 10^{-5}$ m-rad (X),
	0.3 to 0.6 $\times 10^{-5}$ m-rad (Y)
Beam density	$\sim 7 \times 10^{16}$ cm^{-3}

* Work supported in part by the Department of Energy under contracts DE-AC02-76CH03000, DE-AC03-76SF00515, DE-FG03-92ER40695, and DE-FG05-91ER40627, and the Univ. of California Lawrence Livermore National Laboratory, through the Institute for Laser Science and Applications, under contract No. W-7405-Eng-48; and by the US-Japan Program for Cooperation in High Energy Physics.

† Also at UC Davis, Dept. of Applied Science.

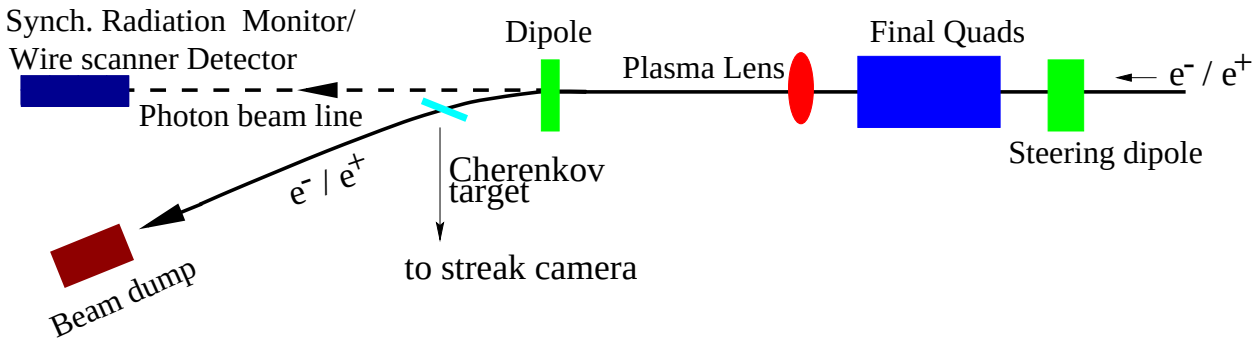

Figure 1: Layout of the plasma lens measurement setup.

3 RESULTS

3.1 *Plasma focusing*

For a bunched relativistic beam traveling in vacuum, the Lorentz force induced by the collective electric and magnetic fields is nearly cancelled, making it possible to propagate over kilometers without significant increase in its angular divergence. In response to the intruding beam charge and current, the plasma electron distribution is reconfigured to neutralize the space charge of the beam and thereby cancel its radial electric field. For a positron beam, the plasma electrons are attracted into the beam volume thus neutralizing it; for an electron beam, the plasma electrons are expelled from the beam volume, leaving behind the less mobile positive ions which neutralize the beam. When the beam radius is much smaller than the plasma wavelength, the neutralization of the intruding beam current by the plasma return current is ineffective because of the small skin depth. This leaves the azimuthal magnetic field unbalanced which then "pinches" the beam. In this experiment, typical plasma densities were of the order of 10^{18} cm^{-3}, corresponding to a plasma wavelength of approximately 30 μm which was indeed much larger than the incoming beam radius.

For data taken with beam self-ionization, the plasma was created when a small fraction of the neutral gas molecules was ionized due to collisions with the high energy beam particles, and the secondary electrons from this impact ionization process were accelerated by the intense collective field in the beam, transverse to the direction of propagation, to further ionize the gas [4]. That is, the head of the bunch was able to ionize the gas while the core and the tail of the bunch were focused.

The results on beam size reduction due to focusing of electron beams by a self-ionization plasma are shown in Figure 2. The transverse beam profile was obtained by measuring the Bremsstrahlung signal as the beam was

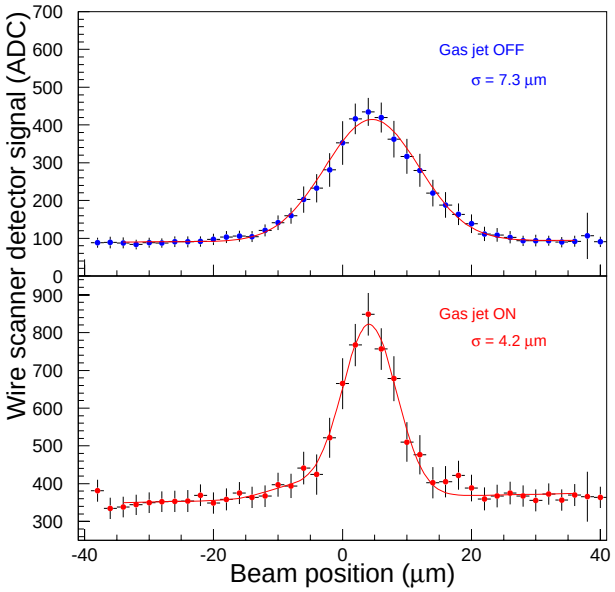

Figure 2: Wire scanner data of transverse beam profile showing focusing of a 29 GeV electron beam by a self-ionization plasma.

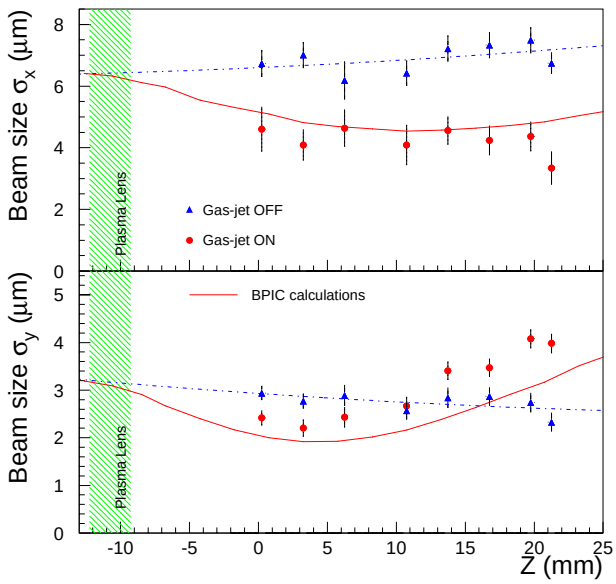

Figure 3: Beam-induced plasma focusing of electron beams. Statistical error only. Results are compared with 3D particles-in-cell simulations.

scanned across the carbon fiber. The wire scanner data were taken with the gas nozzle turned on and off at each beam position, so as to minimize the systematics due to changes in beam conditions when comparing beam sizes measured with and without plasma focusing.

The beam envelope was obtained by measuring the transverse beam size as a function of the downstream distance (Z) of the wire scanner from the plasma lens. The results are shown in Figure 3; a reduction by a factor two in the transverse beam spot area was observed.

Data on focusing by a laser ionized plasma were also collected. The turn-key infrared ($\lambda = 1064$ nm) laser system delivered 1.5 Joules of energy per pulse of 10 ns FWHM at 10 Hz. The laser light was brought to a line focus at the gas jet; the plasma thus produced was approximately 0.5 mm thick as seen by the e^+/e^- beams. With the relatively long infrared laser pulse, the pulse front was able to ionize a small fraction of the gas by multiple-photon absorption; the resulting secondary electrons were accelerated, transverse to the laser's incident direction, to further ionize the gas. This process led to an avalanche growth in plasma density, similar to the beam self-ionization case.

The transverse beam profiles showing focusing of a 29 GeV positron beam by a laser ionized plasma are given in Figure 4. There are several systematic effects in the beam size measurement process. First of all, the carbon-fiber size contributed 1.7 μm to the RMS beam size; this was subtracted in quadrature. Since it took many beam pulses to make a profile measurement, the shot-to-shot jitter in beam centroid position also had an effect. The amount of jitter was estimated to be 25% of the beam size, by measuring the RMS fluctuation at given beam-scan position. When subtracted in quadrature, beam jitter accounted for 6% of the beam size. The positron beam spot was also observed to have a roll angle of 13° with respect to the beam scan direction. The measured transverse beam size was therefore a projection of the true spot size. The effect was negligible except where the aspect ratio of the beam spot was large in which case it was found to be up to 30%.

Because of the strong plasma focusing and the resulting increase in beam divergence, narrow apertures downstream could lead to systematic distortions of the measured beam profile. This effect showed up as an asymmetry in the beam profile, when a portion of the Bremsstrahlung photons were occluded by downstream collimators. The total photon flux, as given by the area under the profile curve, could be reduced by up to 40%. The bunch charge monitored by the toroid just in front of the beam dump showed no loss in beam particles in the plasma lens. The observed asymmetry was also partly the result of beam particles in the tail of the bunch being deflected by wakefields in the linac. The beam profiles were fitted to two half-Gaussians; the larger of the two σ's was taken as the beam size. The accuracy of this procedure was determined using Monte Carlo ray-tracing simulations. The collective fields created

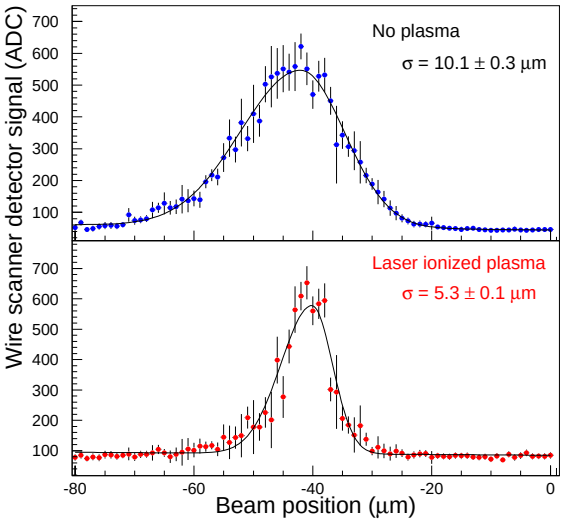

Figure 4: Wire scanner data of transverse beam profile showing focusing of a 29 GeV positron beam by a laser ionized plasma.

by the bunch is [5]:

$$E_y + iE_x = \frac{eN\lambda(z,t)}{4\pi\epsilon_0\sigma_x}\sqrt{\frac{2\pi}{1-r^2}}\Big[w\Big(\frac{x+iy}{\sigma_x\sqrt{2(1-r^2)}}\Big) - exp\Big(-\frac{x^2}{2\sigma_x^2}-\frac{y^2}{2\sigma_y^2}\Big)w\Big(\frac{xr+iy/r}{\sigma_x\sqrt{2(1-r^2)}}\Big)\Big]$$

where $r = \sigma_y/\sigma_x$ is the aspect ratio, $\lambda(z,t)$ the longitudinal bunch distribution, and w is the complex error function. This was used to simulate the the spatial dependence of particle deflection inside a plasma lens. Linear optics was used to simulate the situation without plasma lens. The simulations showed that the beam size measured by fitting two half-Gaussians to an asymmetric profile due to occlusion is within 10% of the true values.

The beam envelope measurements for laser (and beam) ionization plasma focusing of positron beams are shown in Figure 5. In the X-dimension, the beam envelope is shown converging without plasma focusing (square points); while with laser (and beam) induced plasma focusing (filled circles), the beam envelope is shown converging towards a reduced waist and then diverging because of the strong focusing. In the Y-dimension, the waist is at a location close to the the plasma lens beyond the reach of the wire scanner; the beam envelope is seen diverging more rapidly due to the strong plasma focusing.

As shown in previous studies [6], a plasma lens can enhance the luminosity of SLC/NLC type colliders by a factor of five. However, careful design optimization is required. The aberration power describing the phase space dilution

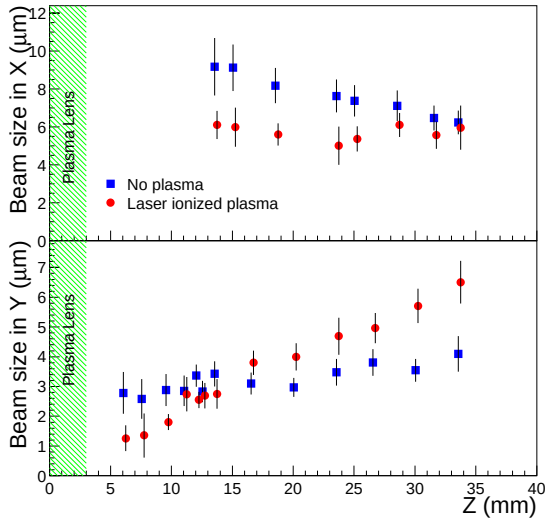

Figure 5: Plasma focusing for positron beams in the X (top) and Y (bottom) dimensions. Errors shown are statistical combined in quadrature with a 10% systematic uncertainty.

by a plasma lens is given for a thin lens by [7]:

$$P = \left[1 + 0.15 \cdot \left(\frac{\beta_0}{f_1}\right)^2\right]^{1/2} \quad (1)$$

where f_1 is the plasma lens focal length. Since the luminosity enhancement would be compromised by a factor P, the β function and the strength of the plasma lens need to be matched to minimize the aberration.

3.2 *Synchrotron radiation induced by plasma focusing*

The synchrotron radiation induced by the strong deflection of beam particles inside the plasma lens provides an independent measure of the plasma focusing strength. It also provides a pulse by pulse diagnostic of the transient plasma lens effect. The critical energy of the emitted synchrotron radiation scales with the strength of the focusing; the synchrotron radiation monitor was designed to measure the penetration profile, which depends on the energy spectrum of the photon flux.

The photon flux detected in the synchrotron radiation monitor contained various background contributions. There was Bremsstrahlung radiation accompanying the beam due to off-axis beam particles interacting with the vacuum chamber wall or upstream collimators, and also synchrotron radiation (with a critical energy $\sim$250 keV) emitted when the spent beam was deflected towards the dump. This was measured with the gas jet turned off and the wire scanner removed from the beam. The contribution from beam-gas Bremsstrahlung, with the gas nozzle turned on, was determined by first measuring the Bremsstrahlung penetration profile from the carbon wire alone, then scaling this profile to the signal measured in the last depth section of the monitor with the beam-associated background removed. After these background contributions were subtracted, an excess in the photon signal beyond a depth of 3 radiation lengths was observed in the electron beam self-ionization plasma focusing data, for nitrogen gas at 550 psi plenum pressure. This excess was not observed when plasma focusing was weak (as determined from beam spot size measurements) for the case of lowered plenum pressure (to below 100 psi, for example), or for the case of hydrogen gas for which beam self-ionization was much less effective.

The penetration profile of the observed signal is consistent with synchrotron radiation with a critical energy of a few MeV according to Monte Carlo simulation. This value corresponds to a focusing gradient of the order of 10^6 T/m, as expected for the plasma lens parameters in this experiment.

3.3 *Laser- and beam-plasma interactions*

Because the laser avalanche ionization process has a finite build-up and decay time, by varying the laser pre-ionization timing before beam arrival at the plasma, different plasma densities can be probed by the high energy beam. The signal in the synchrotron radiation monitor was measured as a function of this advanced timing. Since this signal was predominantly synchrotron radiation induced by plasma lens focusing, the interaction between the high energy beam and the plasma at various stages of formation and decay was monitored. This also means that focusing was observed well into the "after-glow" regime of the laser-induced plasma [9].

The result for positron beams and nitrogen gas at 1050 psi is shown in Figure 6. Time zero corresponded to coincidence between the beam arrival time and the peak of the recombination signal detected in a photomultiplier. The ionization efficiency was measured at time zero also. The synchrotron radiation monitor signal from beam self-ionization plasma focusing was measured at 300 counts (with the laser turned off); the beam-only background signal level was 80 counts (with the gas nozzle turned off).

A quantitative understanding of this delay curve requires detailed modeling of the laser- and beam-plasma interaction process, as well as gas dynamics. A qualitative explanation of this curve is given here. The initial rapid increase in synchrotron radiation monitor signal most likely was due to an increase in plasma focusing strength, peaking at 500 ns. The data shown in Figure 5 were collected with this time delay, when the plasma density had decayed to an optimal level with respect to the beam density. The rapid rise was followed by a sharp decrease to the background signal level of 80 counts. This was predominantly due to an almost complete expulsion of the neutral and ionized gas volume driven by a laser-induced shock wave. Each gas jet pulse, lasting more than 100 μs, supplied a continu-

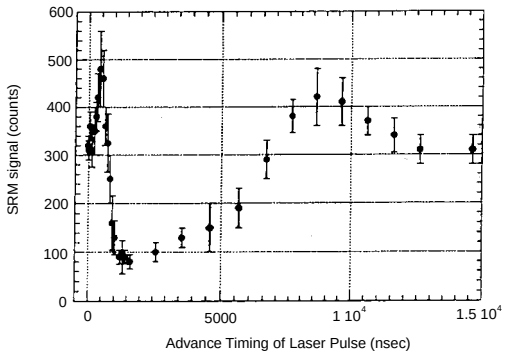

Figure 6: Synchrotron radiation monitor signal (without background subtraction) as a function of the advanced laser ionization timing with respect to beam arrival.

ous stream of neutral gas molecules into the vacuum chamber at sonic speed. Therefore, this abrupt reduction was also assisted by the motion of the plasma, and by its decay. The remainder of the curve starting at 1.5 μs shows a diffusion driven gas recovery phase. Initially, the gas rushed back to fill the void, giving rise to an increased gas density locally above ambient level at 8 μs. During this time, a corresponding rise in beam-ionization plasma focusing signal was observed, on a slow time scale determined by gas dynamics. This was followed by a decay back to local equilibrium level of 300 counts within the time interval 8 to 12 μs. A detailed simulation study should provide further insight into this delay-correlated modulation of plasma focusing.

4 SUMMARY AND OUTLOOK

Results on plasma focusing of 29 GeV electron and, for the first time, positron beams have been presented. Beam self-ionization turned out to be an economical method for producing a plasma lens. The infrared laser with a 10 ns long pulse also proved to be efficient in plasma production, resulting in the strong focusing of electron and positron beams. Data on other aspects of plasma focusing were also collected; detailed discussion is presented elsewhere [10].

Design studies for linear collider applications are just starting. One of the issues being addressed is the effect of beam jitter on the achievable luminosity of plasma focused beams. Optimization of plasma lens parameters requires bench-marking of computer codes as well as better understanding of the various plasma production processes. The experience gained in this experiment will serve as a basis for further engineering design studies for an eventual plasma lens application.

5 REFERENCES

[1] P. Chen, Part. Accel., **20**, 171(1987).

[2] J.B. Rosenzweig *et al.*, Phys. Fluids B **2**, 1376(1990); H. Nakanishi *et al.*, Phys. Rev. Lett, **66**, 1870(1991); G. Hairapetian *et al.*, Phys. Rev. Lett. **72**, 2403(1994); R. Govil *et al.*, Phys. Rev. Lett. **83**, 3202(1999).

[3] V. Balakin *et al.*, Phys. Rev. Lett. **74**, 2479(1995).

[4] R.J. Briggs and S. Yu, LLNL Report UCID-19399, May 1982 (unpublished).

[5] M. Bassetti *et al.*, IEEE Trans. NS-30, No.4, 2182(1983).

[6] P. Chen *et al.*, Phys. Rev. E **48**, No. 4, 3022(1993).

[7] J.B. Rosenzweig and P. Chen, Phys. Rev. D, **39**, No.7, 2039 (1989).

[8] B. Chang *et al.*, Phys. Rev. A **47**, No. 5, 4193(1993).

[9] P. Bolton *et al.*, Proceedings of the 27th IEEE Int. Conf. on Plasma Science, June 2000, New Orleans.

[10] J.S.T. Ng *et al.*, Proceedings of the 9th Advanced Accelerator Concepts Workshop, June 2000, Santa Fe, NM.